



## CFD Simulations Operated by Two Stack Vertical-Axial Wind Turbines for High Performance

Thanaphat Akkarachaiphant<sup>1</sup>, Boonyarit Chatthong<sup>2</sup>, Yutthana Tirawanichakul<sup>2,\*</sup>,  
 Montri Luengchavanon<sup>3,4</sup>

<sup>1</sup> Department of Mechanical Engineering, Faculty of Engineering, Prince of Songkla University, Hatyai, 90110, Thailand

<sup>2</sup> Division of Physical Science, Faculty of Science, Prince of Songkla University, Hatyai, 90110, Thailand

<sup>3</sup> Sustainable Energy Management Program, Wind Energy and Energy Storage Centre (WEESYC), Faculty of Environmental Management, Prince of Songkla University, Hat Yai 90110, Thailand

<sup>4</sup> Center of Excellence in Metal and Materials Engineering (CEMME), Prince of Songkla University, Hat Yai, Songkhla 90110, Thailand

### ARTICLE INFO

#### Article history:

Received 5 January 2022

Received in revised form 15 March 2022

Accepted 16 March 2022

Available online 31 March 2022

#### Keywords:

CFD; Wind energy; Vertical-axis wind turbine (VAWT); Two stack; Coefficient power

### ABSTRACT

Wind energy is a green and sustainable system and vertical axis wind turbines (VAWT) have been developed for low speed operation as small wind turbines. CFD simulations can be conducted to save time and cost. The design structure of the VAWT wind turbine used CFD software for the operation of stream lining. This investigation involved the designs of Model A and B, the Benesh type matched by Model A and the Semicircular type matched by Model B. The CFD simulation compared Cp and TSR values between using Model A and Model B wind turbines. Model A exhibited a 0.24 Cp maximum matched by 1.22 TSR, this model could produce high performance when compared to Model B. Model A could be increased by 4.8 times the Cp value when compared with Model B. The 3D velocity streamlines and corresponding vector plots at various angular positions can be performed using the wind flow with corresponding Cp values.

## 1. Introduction

Wind energy is environmentally a component of renewable energy that is available all around the world. Micro-wind turbines have become more popular in urban areas, although the high turbulence of wind flow needs to be considered as the wind flow in such environment is affected by pressure change. The main point is not only the high turbulence intensity but also huge velocity fluctuations with large vertical components caused by the existence of buildings. The challenges are based on the swiftly changing wind directions in urban areas which have been studied [1]. Many variations involved the wind negatively affecting the activation of all types of wind turbines. Highly fluctuating winds have been proposed as a solution for harvesting wind energy [2], such as by focusing on vibration driven by the wind current [3]. The vibrations devices generated from the different flow-

\* Corresponding author.

E-mail address: [yutthana.t@psu.ac.th](mailto:yutthana.t@psu.ac.th) (Yutthana Tirawanichakul)

induction that used hybrid piezoelectric wind energy scavengers have been developed with 71% high efficiency power [4]. Meanwhile, the development of low speed wind turbines has been improved to harvest all of the range of wind currents by designing new blades, reducing the starting torque of the electrical generator, ensuring low friction of bearings, and so forth [5, 6].

In the mid-90s the pilot programmes started on vertical axis wind turbines (VAWTs) for generating electricity [7]. The different wind turbine architectures can form the structure. The Savonius rotor is easily installed with small structure where effective self-starting is required in hydrokinetic applications [8, 9]. On the other hand, the Darrieus rotors are offered as a convenient alternative to horizontal axis wind turbines (HAWTs) for power generation which can be used in small and medium sized applications [10]. Darrieus rotors have improved performance independent of wind direction and wind mass concentration at the ground, allowing highly effective control of the system oscillations. Additionally, VAWTs are preferred over other turbine types in densely populated areas due to this turbine being perceived as aesthetically more beautiful, and easier to install in the terrain [11]. However, different designs can be available for a specific type of rotor in terms of number of blades, materials, shapes and strut types.

Generally, the experimental investigation is often highly costly, but Computational Fluid Dynamics (CFD) can simulate the experiment in a versatile and accurate manner to develop the investigation of Savonius and Darrieus VAWT air flow aerodynamics and can provide high performance in VAWTs design. CFD can provide the development of computationally highly efficient algorithms or dedicated codes [12].

This research study the performance of wind turbines via computational fluid dynamics (CFD) by using the program ANSYS® Fluent which is widely used for the study of fluids such as water and air. Many previous studies of VAWT wind turbines were based on the use of 2D CFD models and some studies were based on the use of 3D CFD models. Other studies used an experimental approach for the performance analysis and improvements. The wind turbines that were used for this study were two stacks Savonius wind turbine model, a Savonius rotor with two stacks and connected Darrieus rotor which can improve the performance of the VAWT wind turbine. Therefore, this study mainly focus on using 3D CFD to find the performance of the designed wind turbines with dynamic mesh method by using material info to determine the properties. The experimental measurement are used to support the simulation results from the CFD. The result of this study could prove the usefulness of CFD to design and develop for the future wind turbine.

## 2. Simulation of the Wind Turbine and Wind Tunnel Experiment

Commonly, the general parameter in the technology of wind turbines can be reviewed. The power available ( $P_{Wind}$ ) from the natural wind flow for cross-section area ( $A_s$ ) is provided by:

$$P_{Wind} = 0.5\rho(A_s)V^3 \quad (1)$$

where  $\rho$  is the density of the air and  $V$  is the wind speed. Based on the vertical axis wind turbine, the swept area ( $A_s$ ) is formed into a rectangle that can be calculated as the turbine diameter multiplied by the blade length. Meanwhile the power coefficient is the measurement of the wind turbine's ability to transfer wind energy to mechanical energy that is defined as:

$$C_p = \frac{P_{Wind\ turbine}}{P_{Wind}} \quad (2)$$

where  $P_{Wind\ turbine}$  is the output of aerodynamic power from the wind turbine. Generally, the relationship of the wind turbine representing the power coefficient depends on the tip speed ratio TSR or  $\lambda$  that indicates the ratio between the velocity of the blade and the wind speed, hence calculated as:

$$\lambda = \frac{\omega R}{V} \quad (3)$$

where  $\omega$  represents the angular velocity of the turbine and  $R$  represents the turbine radius.

3D simulation with ANSYS® Fluent, in mesh setting with an unstructured triangular mesh is applied to discretize the whole domain with the element size of 0.01 m linear element order. In this part of the domain, a logarithmic law of the wall is applied.

In order to allow the physical revolution and rotation of the turbine, the dynamic mesh method is used for the solver. Turbulent flow is modelled using a Reynolds-Averaged version of continuity and Navier-Stokes equations and transport equations for turbulence quantities. The turbulence model for this simulation is k- $\omega$  standard. The solver is transient for the incompressible flow of Newtonian fluids on a moving mesh. In the boundary condition the inlet will have input at 5 m/s velocity and 1.225 kg/m<sup>3</sup> operating density. To find the solution with the dynamic mesh method we have to set the parameter to define the six DOF which are moment of inertia and center axis of the wind turbine, where the moment of inertia depends on the material that is used for reference in the wind turbine.

The VAWT models that were used for the simulation are shown in Figure 1. Figure 1 (a) shows Model A, fabricated from 2 Savonius blades stacked together. The upper and lower blades were cross-deposited at 90 degrees. At the end of the Savonius blades were 20 degree bent curves [13]. Figure 1 (b) shows Model B that has 3 Savonius blades stacked together and the curve of the blades was fabricated by using a half circle of 5 cm radius. The upper and lower parts were cross-deposited with space between the blades.

Figure 2 shows the wind tunnel experimental testing setup for comparison with the CFD simulation results. Note that the blades were fabricated using acrylic materials. Figure 2 (a) shows the 1hp motor and wind speed flow controller that can produce wind flow speeds of 0-6 m/s. Experimentally, the GM 8903 Hot Wire Anemometer was used to measure the wind speed, the DIGITION PHOTO TACHOMETER (DT-2234C<sup>+</sup>) was used to measure revolution, and the torque meter, DRBK-A with range 100N-m<sub>2</sub> was used to measure the torque. Figure 2 (b) shows the middle section of size 3.0 x 0.3 m<sup>2</sup> where the A and B VAWT models can be inserted to measure the rotation and torque. The properties of the VAWT wind turbines are shown in Table 1. Note that the acrylic materials were generated for simulation with mass and moment of inertia of 235 g and 0.92 m<sup>2</sup>, respectively.

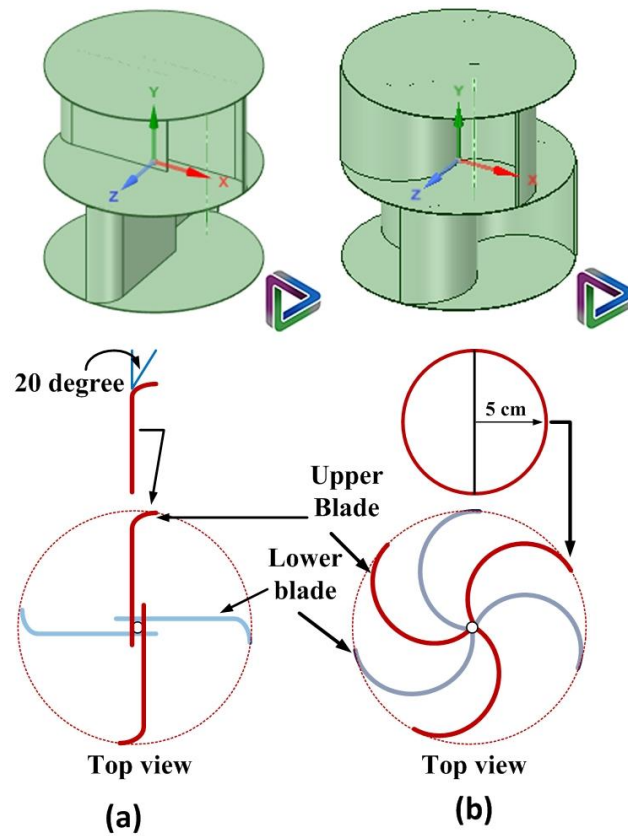


Fig. 1. VAWT created into the Model A (a) and Model B (b)

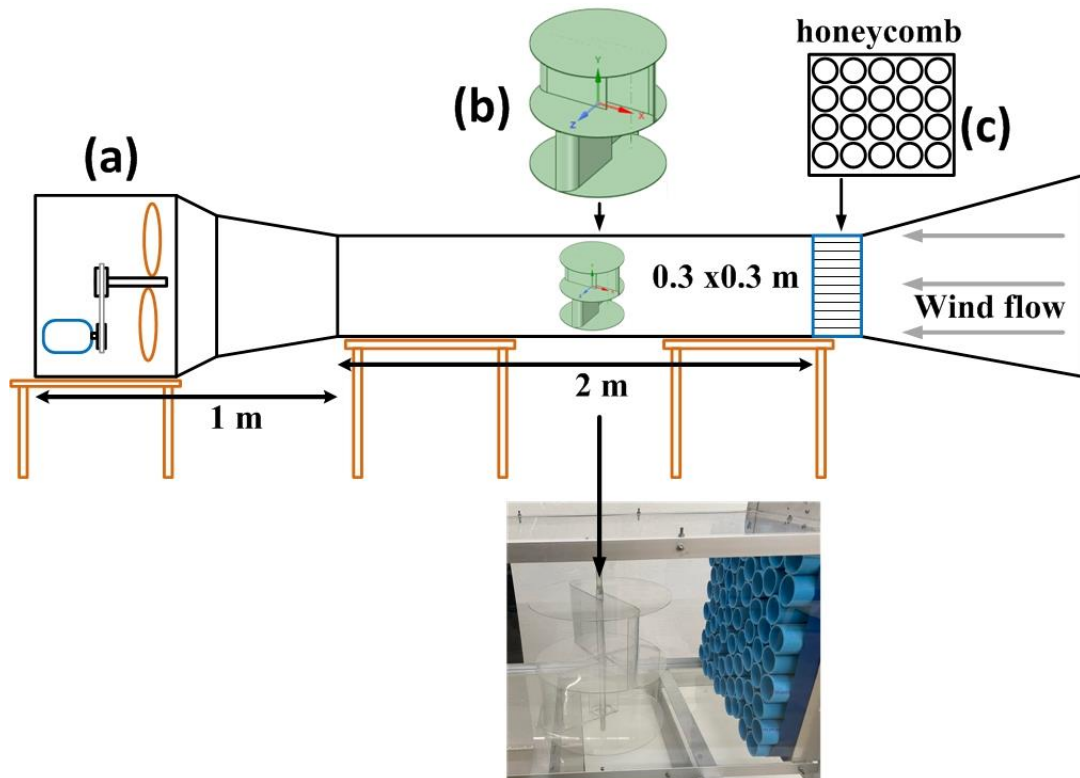


Fig. 2. Wind tunnel experiential VAWT testing for comparison with CFD simulation results

**Table 1**  
 Properties of the A model VAWT wind turbine

Properties of the VAWT wind turbine	Specification
Number of blades	2x2 (stack)
Height	20 cm
Radius	10 cm
Blade thickness	0.15 cm
Plate thickness	0.1 cm
Gap between two blades	2 cm
Centre pole diameter	1 cm

### 3. Results

Figure 3 shows the results of CFD simulation showing the relation between  $C_p$  and TSR, using Model A and Model B wind turbines. Model A exhibited a 0.24  $C_p$  maximum matched by 1.22 TSR. This model can provide higher performance compared to Model B. Meanwhile Model B indicated a 0.05  $C_p$  maximum matched by 0.6 TSR. Model A clearly yields 4.8 times the  $C_p$  value to that of Model B. Figure 4 shows the structure of VAWT blade profiles, in which Figure 4(a) shows the Semicircular type that is matched by Model B, while Figure 4 (b) shows the Benesh type which is matched by Model A in this investigation. The numerical variations of  $C_p$  for the Semicircular type are observed to be 0.272 at TSR = 0.8; whereas at the same TRS, the peak  $C_p$  is indicated to be 0.294 for the Benesh type [14]. Based on Figure 4, the magnitude of high velocity is revealed near the surface of the advancing of the Benesh type. The overlapping flow is found to be more significant in the Benesh type than the Semicircular type [14, 15]. Additionally, the effect of the end-bent airfoil on the blades of the axial compressor indicated that surge margin is elevated by 4.9-5.2% with efficiency promoted by 2.6-3.2% at operational speed [16]. The application of end-bends at the wing or blade can reduce the suction surface (SS) corner stall [17]. Therefore, Model A can generate greater  $C_p$  than Model B.

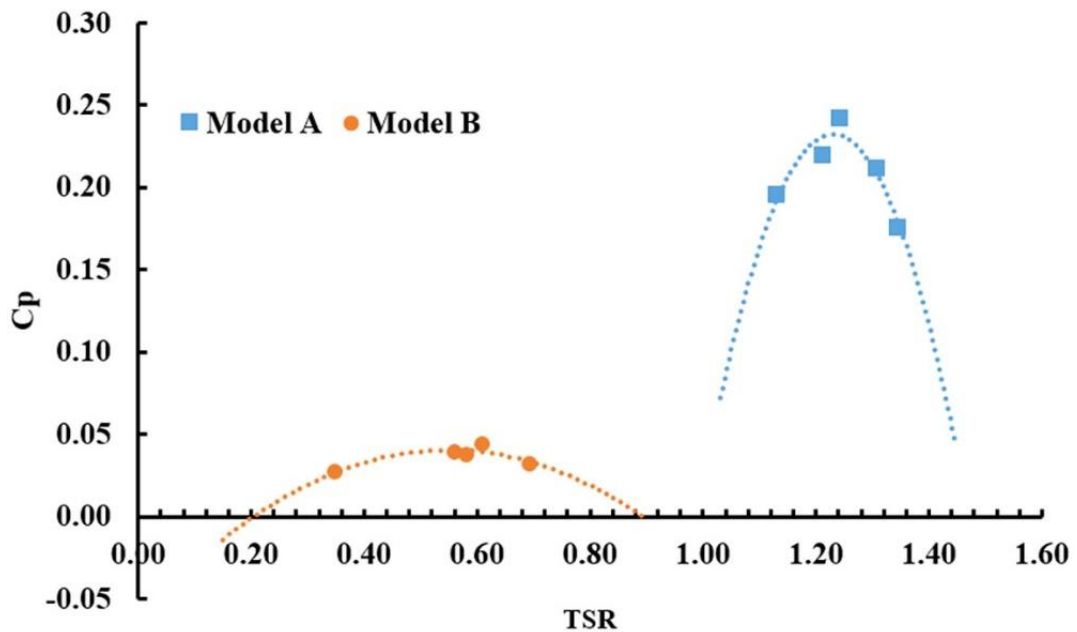


**Fig. 3.** The operation of Model A and Model B VAWT wind turbines demonstrating the power coefficient ( $C_p$ ) versus tip Speed Ratio (TSR)

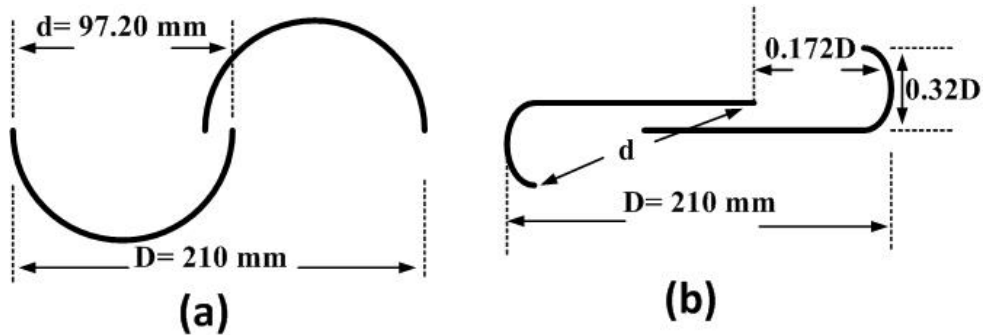


**Fig. 4.** Structure of various VAWT blade profiles, (a) Semicircular type (b) Benesh type [14]

Figure 5 shows the comparison of relation between  $C_p$  and TSR properties between VAWT simulation and experimental results using Model A. The result from the simulation of Model A revealed that the 0.24  $C_p$  maximum was matched by 1.22 TSR. At the same TSR, the experimental Model A can operate at 0.23  $C_p$  maximum. These values agreed quite well with less than 5% difference. On the other hand, the range of TSR between simulation and experiment showed different values whereby the range for the experimental Model A is wider than the simulation. Generally, the power coefficients of Savonius rotors comprise  $C_p$ . For the experimental study, the rotor torque ( $T$ ) is tested by multiplying the load ( $F$ ) given to the pulley adjoining the rotor and radius of the pulley ( $r$ ). Therefore, the  $C_p$  are represented as shown in Eq. (2) but the  $P_{windturbine}$  can be calculated as in Eq. (4) [18] which clearly separated the factors of power from the VAWT wind turbine.

$$P_{windturbine} = T(\omega_s) = \frac{2\pi NT}{60} \tag{4}$$

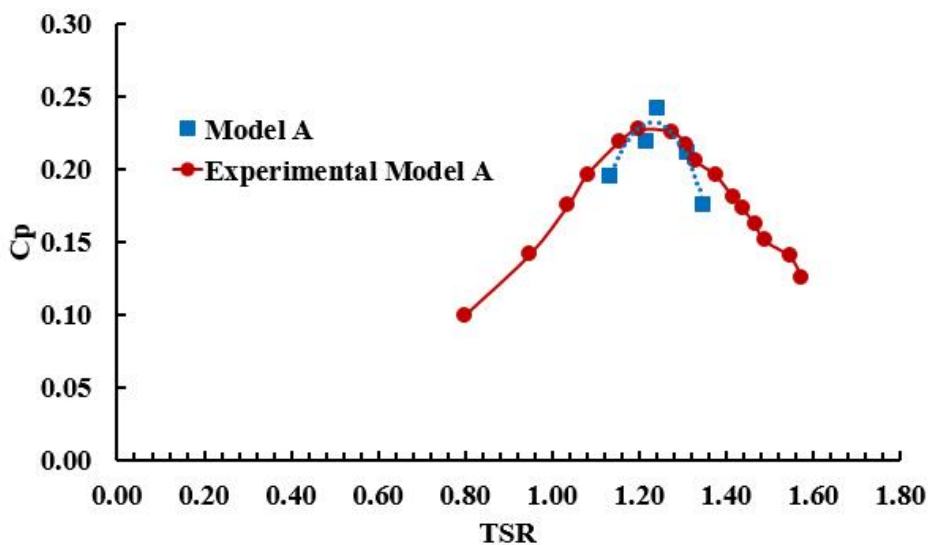


**Fig. 5.** Comparison of  $C_p$  and TSR properties between VAWT simulation and experimental results using Model A

Note that  $T$  represents the torque generated by the rotor (N·m),  $\omega_s$  is rotor rotational speed (rad/s) and  $N$  is the rotational speed of the rotor (rpm). The  $T$  factor is a fluctuating value caused by

the friction from bearings and the inertia force from the accessories of the VAWT wind turbine. Additionally, the wind tunnel blockage ratio (BR) can be a generated factor that needs to be investigated while operating the VAWT wind turbine [19]. The new correlation for blockage corrections in the Savonius wind turbine should operate in the open type section [20], where the blockage corrections factor ( $f$ ) is provided to correct the investigated parameters such as the rotational speed of the turbine ( $N$ ), wind speed ( $V$ ) and mechanical load applied to the turbine ( $F$ ) [20]. Based on the blockage correction factor,  $f=4-9\%$  is promoted relating to various BR and TSRs of 21.16% [19, 20]. The results from experimental Model A showed a wider range of TSR than the simulation results. This was produced from BR values because this value can affect many factors of VAWT wind turbines.

The streamline and vector plots of the crosswind turbine of Model A are simulated in Figures 6-8 at different angular positions. Figure 6 (a) shows the top view of the streamline flowing through the gap and the end-bends of blades; the image can be interpreted from the absence of small vortices downstream of the returning blades activating in the conventional VAWT wind turbine, as the flow initially generates a pressure area [21]. Figure 6 (b) shows the side view of the streamline flow through the blades and the green lines are across the blades. Figure 7 (a) shows an image fabricating crosswind flow stream across advancing blades that can be a smoothed flow on the upstream of the returning blades, shrinking the high pressure area [21, 22]. Figure 7 (b) shows the side view of the streamline flow through the blades and the green lines are highly crossing the blades. Figure 8 (a) shows that the stream reduces the pressure on the upstream side of the advancing blades, hence weakens the crosswind stream and allows for a higher pressure on the advancing blade [23]. The returning blade wake vortices cannot attack the wake of the advancing blade that explains the location of the circle when producing high pressure on the downstream surface of the advancing blade [24]. Figure 8 (b) shows the side view of the streamline flowing through the blades and the green lines are highly crossing the blades, represented obviously by the shape of the yellow and green lines depending on the velocity and pressure.

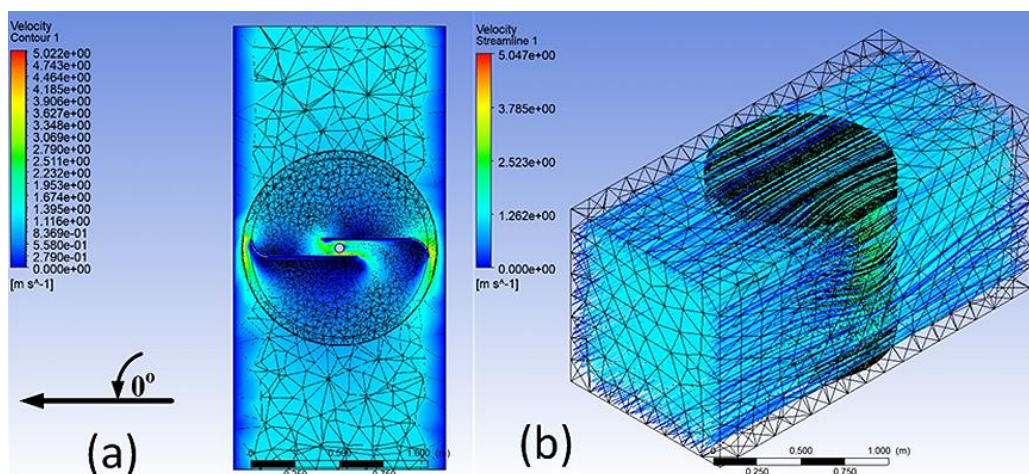


**Fig. 6.** 3D velocity streamlines and corresponding vector plots at angular position  $0^\circ$  and meshes for CFD models. (a) top views of illustrations are planar, referring to the mid-turbine plane and are limited to the rotating zone; (b) perspective illustrations are side view, referring to the edge-turbine plane, and are limited to the rotating

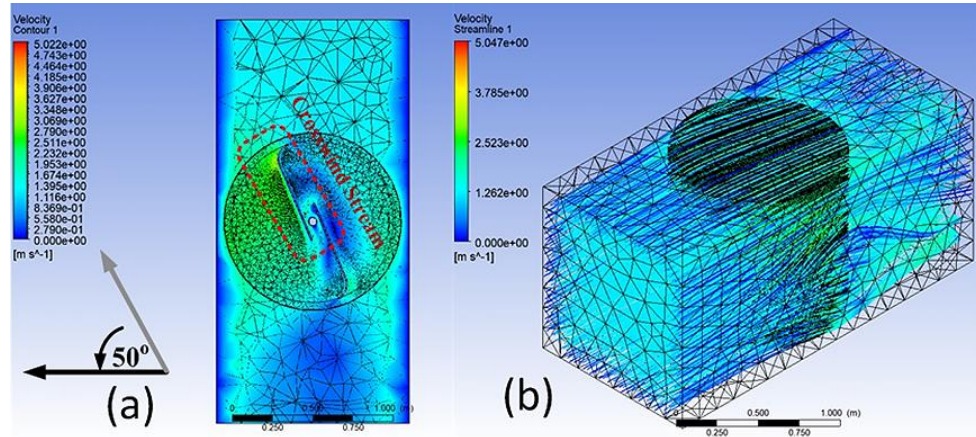


**Fig. 7.** 3D velocity streamlines and corresponding vector plots at angular position 50° and meshes for CFD models. (a) top views of illustrations are planar, referring to the mid-turbine plane, and are limited to the rotating zone; (b) perspective illustrations are side view, referring to the edge-turbine plane and are limited to the rotating zone

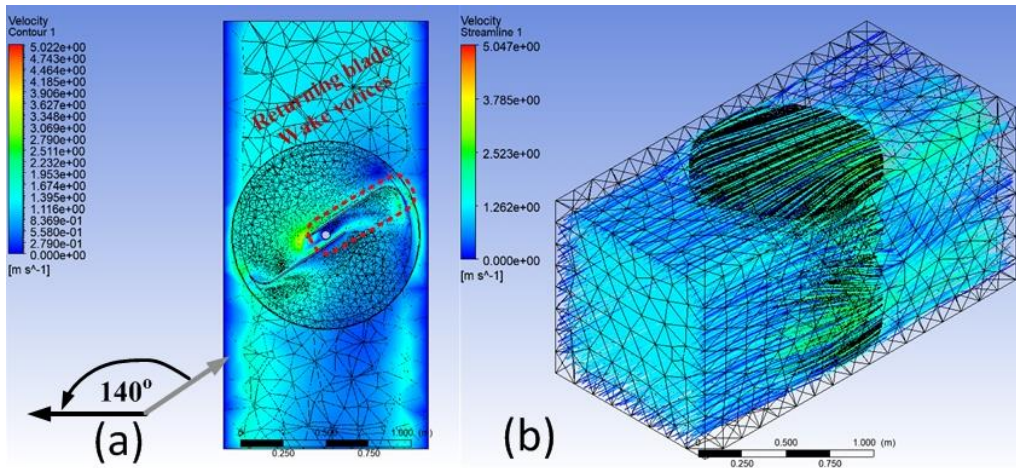


**Fig. 8.** 3D velocity streamlines and corresponding vector plots at angular position 50° and meshes for CFD models. (a) top views of illustrations are planar, referring to the mid-turbine plane, and are limited to the rotating zone; (b) perspective illustrations are side view, referring to the edge-turbine plane, and are limited to the rotating zone

#### 4. Conclusions

The VAWT wind turbine is one technology for renewable energy that can be continuously developed for small wind energy. The Savonius blades have been designed in many form for the low speed wind turbines, and the stacked Savonius blades have been also designed as a structure that can achieve high performance for a VAWT wind turbine. CFD simulations can reduce the cost and time for production of the structure of the turbine. The design structure of the VAWT wind turbine used CFD software for the operation of the stream-lining. This investigation was designed using Models A and B, in which the Benesh type was matched by Model A and the Semicircular type was matched by Model B. The results of the CFD simulation compared  $C_p$  and TSR, using Model A and Model B wind turbines. Model A exhibited a 0.24  $C_p$  maximum matched by 1.22 TSR; this model can provide higher performance when compared to Model B. Meanwhile, Model B merely indicated a 0.05  $C_p$  maximum matched by 0.6 TSR. Model A can be clearly increased by 4.8 times the  $C_p$  value

when compared to Model B. Model A was chosen as an experimental test and validated the Cp value. The comparison of the CFD simulation and experimental Model A indicated that range of TSR was difference. The experimental Model A shows the TSR range of values wider than that of the CFD simulation. When the 3D velocity streamlines and corresponding vector plots at various angular positions were performed, the positions generated the pressure from the wind flow with corresponding Cp values. Therefore, CFD simulation can be performed for designing VAWT wind turbines to save both time and cost for the estimation of wind power.

### Acknowledgement

The authors would sincerely like to thank to Graduate school, Department of Mechanical Engineering, Faculty of Engineering and Department of Physics, Faculty of Science on Prince of Songkla University for their support and experiment space, and Interdisciplinary Graduate School of Energy System (IGS-Energy) for their financial support.

### References

- [1] Anup, K. C., Jonathan Whale, and Tania Urmee. "Urban wind conditions and small wind turbines in the built environment: A review." *Renewable energy* 131 (2019): 268-283. <https://doi.org/10.1016/j.renene.2018.07.050>
- [2] Zou, Hong-Xiang, Lin-Chuan Zhao, Qiu-Hua Gao, Lei Zuo, Feng-Rui Liu, Ting Tan, Ke-Xiang Wei, and Wen-Ming Zhang. "Mechanical modulations for enhancing energy harvesting: Principles, methods and applications." *Applied Energy* 255 (2019): 113871. <https://doi.org/10.1016/j.apenergy.2019.113871>
- [3] Han, Nuomin, Dan Zhao, Jorg U. Schluter, Ernest Seach Goh, He Zhao, and Xiao Jin. "Performance evaluation of 3D printed miniature electromagnetic energy harvesters driven by air flow." *Applied energy* 178 (2016): 672-680. <https://doi.org/10.1016/j.apenergy.2016.06.103>
- [4] Wang, Junlei, Shanghao Gu, Chengyun Zhang, Guobiao Hu, Geng Chen, Kai Yang, Hang Li, Yuyang Lai, Grzegorz Litak, and Daniil Yurchenko. "Hybrid wind energy scavenging by coupling vortex-induced vibrations and galloping." *Energy Conversion and Management* 213 (2020): 112835. <https://doi.org/10.1016/j.enconman.2020.112835>
- [5] Trongtorkarn, Mintra, Thanansak Theppaya, Kuaanan Techato, Montri Luengchavanon, and Chainuson Kasagepongsarn. "Relationship between Starting Torque and Thermal Behaviour for a Permanent Magnet Synchronous Generator (PMSG) Applied with Vertical Axis Wind Turbine (VAWT)." *Sustainability* 13, no. 16 (2021): 9151. <https://doi.org/10.3390/su13169151>
- [6] Ngoc, Duong Minh, Kuaanan Techato, Le Duc Niem, Nguyen Thi Hai Yen, Nguyen Van Dat, and Montri Luengchavanon. "A Novel 10 kW Vertical Axis Wind Tree Design: Economic Feasibility Assessment." *Sustainability* 13, no. 22 (2021): 12720. <https://doi.org/10.3390/su132212720>
- [7] Möllerström, Erik, Paul Gipe, Jos Beurskens, and Fredric Ottermo. "A historical review of vertical axis wind turbines rated 100 kW and above." *Renewable and Sustainable Energy Reviews* 105 (2019): 1-13. <https://doi.org/10.1016/j.rser.2018.12.022>
- [8] Altan, Burcin Deda, and Mehmet Atilgan. "An experimental and numerical study on the improvement of the performance of Savonius wind rotor." *Energy Conversion and Management* 49, no. 12 (2008): 3425-3432. <https://doi.org/10.1016/j.enconman.2008.08.021>
- [9] Sarma, Neelam K., Agnimitra Biswas, and Rahul D. Misra. "Experimental and computational evaluation of Savonius hydrokinetic turbine for low velocity condition with comparison to Savonius wind turbine at the same input power." *Energy conversion and management* 83 (2014): 88-98. <https://doi.org/10.1016/j.enconman.2014.03.070>
- [10] Tjiu, Willy, Tjukup Marnoto, Sohif Mat, Mohd Hafidz Ruslan, and Kamaruzzaman Sopian. "Darrieus vertical axis wind turbine for power generation I: Assessment of Darrieus VAWT configurations." *Renewable energy* 75 (2015): 50-67. <https://doi.org/10.1016/j.renene.2014.09.038>
- [11] Hamdan, A., F. Mustapha, K. A. Ahmad, and AS Mohd Rafie. "A review on the micro energy harvester in Structural Health Monitoring (SHM) of biocomposite material for Vertical Axis Wind Turbine (VAWT) system: A Malaysia perspective." *Renewable and Sustainable Energy Reviews* 35 (2014): 23-30. <https://doi.org/10.1016/j.rser.2014.03.050>
- [12] F. Balduzzi, A. Bianchini, F. Gigante, G. Ferrara, M.S. Campobasso, L. Ferrari, in, 2015.
- [13] Li, Zhihui, and Yanming Liu. "Blade-end treatment for axial compressors based on optimization method." *Energy* 126 (2017): 217-230. <https://doi.org/10.1016/j.energy.2017.03.021>

- [14] Roy, Sukanta, and Ujjwal K. Saha. "Wind tunnel experiments of a newly developed two-bladed Savonius-style wind turbine." *Applied Energy* 137 (2015): 117-125. <https://doi.org/10.1016/j.apenergy.2014.10.022>
- [15] Asadi, Mohammad, and Rahim Hassanzadeh. "On the application of semicircular and Bach-type blades in the internal Savonius rotor of a hybrid wind turbine system." *Journal of Wind Engineering and Industrial Aerodynamics* 221 (2022): 104903. <https://doi.org/10.1016/j.jweia.2022.104903>
- [16] Y.J. Cai, Y.L. Zhong, L.H. Qian, S.Z. He, Q.H. Pang, in: ASME 1985 Beijing International Gas Turbine Symposium and Exposition, 1985.
- [17] C.J. Robinson, J.D. Northall, C.W.R. McFarlane, in: ASME 1989 International Gas Turbine and Aeroengine Congress and Exposition, 1989.
- [18] Kamoji, M. A., S. B. Kedare, and S. V. Prabhu. "Performance tests on helical Savonius rotors." *Renewable Energy* 34, no. 3 (2009): 521-529. <https://doi.org/10.1016/j.renene.2008.06.002>
- [19] Abraham, J. P., B. D. Plourde, G. S. Mowry, W. J. Minkowycz, and E. M. Sparrow. "Summary of Savonius wind turbine development and future applications for small-scale power generation." *Journal of Renewable and Sustainable Energy* 4, no. 4 (2012): 042703. <https://doi.org/10.1063/1.4747822>
- [20] Roy, Sukanta, and Ujjwal K. Saha. "An adapted blockage factor correlation approach in wind tunnel experiments of a Savonius-style wind turbine." *Energy Conversion and Management* 86 (2014): 418-427. <https://doi.org/10.1016/j.enconman.2014.05.039>
- [21] Chemengich, Sammy Jamar, Sadek Z. Kassab, and Eslam R. Lotfy. "Effect of the variations of the gap flow guides geometry on the savonius wind turbine performance: 2D and 3D studies." *Journal of Wind Engineering and Industrial Aerodynamics* 222 (2022): 104920. <https://doi.org/10.1016/j.jweia.2022.104920>
- [22] Elsayed, Ahmed M. "Design Optimization of Diffuser Augmented Wind Turbine." *CFD Letters* 13, no. 8 (2021): 45-59. <https://doi.org/10.37934/cfdl.13.8.4559>
- [23] Niknahad, Ali. "Numerical study and comparison of turbulent parameters of simple, triangular, and circular vortex generators equipped airfoil model." *Journal of Advanced Research in Numerical Heat Transfer* 8, no. 1 (2022): 1-18.
- [24] Alom, Nur, and Ujjwal K. Saha. "Influence of blade profiles on Savonius rotor performance: Numerical simulation and experimental validation." *Energy Conversion and Management* 186 (2019): 267-277. <https://doi.org/10.1016/j.enconman.2019.02.058>